JPMTR 070 | 1503
DOI 10.14622/JPMTR-1503
UDC 539.6 – 035.67 : 763

Original scientific paper
Received: 2015-06-23
Accepted: 2015-11-17

Ink adhesion failure during full scale offset printing: causes and impact on print mottle

Hajer Kamal Alm[1], Göran Ström[1], Joachim Schoelkopf[2], Cathy Ridgway[2] and Patrick A. C. Gane[2]*

[1] Innventia AB,
BOX 5604, SE-114 86 Stockholm, Sweden
[2] OMYA Development AG, P.O BOX: 32,
CH-4665 Oftringen, Switzerland
[*] (also) Aalto University, School of Chemical Technology,
P.O. Box 16300, FI-00076 Aalto, Finland

E-mails: hajer.kamal@innventia.com
goran.strom@innventia.com
joachim.schoelkopf@omya.com
cathy.ridgway@omya.com
patrick.gane@omya.com

Abstract

The printing plate used in offset lithography is designed to accept ink on image areas and reject ink on non-image areas. In order to reject ink in conventional offset, fountain solution is needed to form a weak boundary layer between the plate and the ink. Paper and coated paper in particular are designed to accept ink and absorb ink oil and fountain solution. The latter is often transferred to the paper surface through the rubber blanket and its absorption or subsequent displacement is essential for final ink transfer to the surface. There are strong demands on the uniformity of the paper surface, including in respect to absorptivity, both in structure and chemistry, in order to gain a print of high quality. If this is not the case, the ink film thickness may be non-uniform; subsequently, ink adhesion may even fail completely, leaving white spots on the paper surface in the print. This gives rise to print mottle, a severe print quality defect.

The aim of this paper was to study the quality of prints from a full scale offset printing trial made on pilot coated paper, with attention given to ink-surface adhesion. Seven calcium carbonate pigment based coatings with different contents of pigment dispersing agent were included in this study. The work showed that a moderate over-dosage of dispersant significantly increased the ink adhesion failure and print mottle, mainly on prints from the later print units and especially at high fountain feed levels. These findings demonstrate the fundamental impact of fount level, surface chemistry and coating formulation on ink adhesion and thus also print mottle.

Keywords: coated paper, coating permeability, offset print quality, water induced print mottle, uncovered area, polyacrylic dispersant

1. Introduction

The principal function of fountain solution in conventional offset printing is to prevent ink to be transferred to the non-image areas of the printing plate (MacPhee, 1979; Kipphan, 2001). The fountain feed level is a delicate control issue for the printer. Too low a feed volume will cause scumming, i.e. the non-image areas will take up ink and start to print. Too high a feed will give problems with poor ink transfer and print quality defects will appear. A minimum thickness of the fountain film is considered to be around 40 to 80 nm (see Discussion for details), which is well below the range of 0.5–1 μm which has been reported as a normal average thickness (MacPhee, 1979). However, the non-image area of the plate is not mirror-smooth, a press design feature is applied to ensure satisfactory fount transfer, and so sufficient fountain feed is needed in order to assure that the water film on elevated areas also has an appropriate thickness.

Both ink and paper must be compatible with fountain solution in order to assure ink transport in the press and good print quality. The ink must be able to incorporate fountain solution in a water-in-oil emulsion (MacPhee, 1979; Fadner and Doyle, 1985). Also the paper needs to cater for water that has been deposited on its surface when the paper comes into contact with water rich regions on the rubber blanket. The water is first hydraulically impregnated into the paper in the nip in a process controlled by the paper permeability and then subsequently capillary absorbed by the top layer of the paper during the time that elapses between two nips (Aspler, 2006). Direct measurements of water uptake by coated papers during heatset offset printing have been reported by Tåg et al. (2010, 2011). They used near infra-red probe spectroscopy and confirmed a significant water uptake which was influenced by coating smoothness and

capillarity. Due to the high speed of the printing process, the controlled uptake of water into ink and paper must be fast. Compact areas of the paper surface have a low capability to remove larger water volumes fast enough from the surface and this will give problem with ink transfer to the paper.

Print mottle is a perceived uneven print density and a common and severe print defect on coated papers. The amount of wet ink transferred to the paper is very low, less than 1 $g \cdot m^{-2}$ (MacPhee and Lind, 1991) and after drying when the ink oil has depleted from the ink film (Ström and Gustafsson, 2006), the thickness of the dry ink film (i.e. pigment and binder) is in the order of half a micrometre or less (Ström and Karathanasis, 2008). Thus, it is easy to understand that a very small variation in ink film thickness and small spots were the ink has failed to adhere to the surface will result in a mottled low quality print.

There are two principal types of print mottle. Back trap mottle (BTM) is due to variation in ink film thickness. This mottle type has been subjected to scientific studies in both laboratories and on printing presses for half a century, with significant breakthroughs seen during the last 10–15 years (Ozaki, Bousfield and Shaler, 2008; Rajala and Koskinen, 2004; Xiang et al., 2000; Shen et al., 2005; Xiang et al., 1999; Isoard, 1983). BTM is basically due to an uneven depletion of ink oil by transfer into the coating, which in turn is due to a non-uniform pore structure and/or surface chemistry of the coating. This results in an ink film on the paper with local variations in thickness and viscosity. This gives an uneven build-up of ink on the non-image areas of the rubber blanket and non-uniform ink transfer (back trap) in subsequent print units where the previous printed area meets the non-image area of the following rubber blanket, and finally a non-uniform ink film thickness on the paper that exits the printing press.

The other principal type of mottle is water interference mottle (WIM) (Plowman Sandreuter, 1994). Only very little scientific work in this area have been reported (Ström and Madstedt, 2009; Lie and Kolseth, 2007). The common belief is that it is due to ink refusal caused by too high a fountain solution feed rate. We became interested in this research area after a laboratory study on ink adhesion (Kamal et al. 2010; Kamal Alm et al., 2010), where we realised that ink adhesion failure could have several origins. Not only fountain solution feed was important but also paper properties and the interaction between fountain solution and paper coating.

The laboratory work (Kamal et al. 2010; Kamal Alm et al., 2010) showed that an excess amount of sodium polyacrylate in the coating colour affected the coating properties and the interaction between ink and the paper coating. The coatings became more polar and interacted more strongly with water. This resulted in slower ink setting and reduced ink–paper coating adhesion, especially in the presence of applied water/dampening solution (to mimic fountain solution during offset printing) which are identified as contributory factors in ink piling and print mottle (Purfeerst and Van Gilder, 1991). The work showed that ink adhesion failure resulted in white spots in the print and suggested that the ink failure was due to two different mechanisms, the well-known ink refusal, which is an ink transfer failure, and a new mechanism, which we refer to as ink-lift-off. The latter mechanism suggests that the ink is transferred to the paper surface but removed in a subsequent print nip due to poor ink-surface adhesion (Kamal Alm et al., 2015).

In order to verify if the findings from the laboratory study had any relevance in industrial printing, we designed a special pilot coating trial and printed the coated papers in full-scale sheet-fed offset with a layout designed for our aims. The results are reported in two articles. The first (Kamal Alm et al., 2015) focuses on the impact of paper coating properties gained from the size distribution of the pigment, type of latex binder, calendering and one dosage of additional dispersant on ink adhesion failure. The white spots that were a result of ink adhesion failure were analysed in detail, the unprinted surfaces were inspected with scanning electron microscopy (SEM) and a mechanism was proposed. Now, the second report, i.e. this paper, focuses on paper properties that arise from the use of high amounts of dispersant since this appears to be a key factor, and especially since paper mills often add in extra dispersant(s) to the colour in order to assure that it will perform well on the coater following, for example, pH shock in the case of calcium carbonate, arising frequently from the use of acidic binders or microbiological contamination on the machine. Both reports focus on fountain solution/water feed in addition to paper properties on ink adhesion and print quality. The present paper additionally discusses print quality properties in more detail.

2. Materials and methods

2.1 Coating colour formulations

Seven different coating colours were formulated. The coatings were prepared according to the formulations in Table 1. The same pigment, a ground calcium carbonate (GCC) with mass fraction of 90 % of the particles being less than 2 μm, was used in all formulations. The GCC pigment (Hydrocarb 90, supplied by OMYA) was delivered in the form of dispersed slurry where polyacrylate (PA) dispersant had been used during its

production. The binder used in all formulations was a styrene-butadiene latex (DL920 supplied by STYRON).

The additional polyacrylic dispersant used for excess dosing was Dispex N40 (supplied by BASF), a fully sodium neutralised dispersant (NaPA). The NaPA solution used in the experiment consisted of diluted commercial product, in which only water had been added. A further dispersant solution was also prepared, a partially calcium neutralised (NaCaPA). In the NaCaPA solution a calcium to acrylate ratio ($[Ca^{2+}]/[A^-]$) of 0.3 was targeted. The ion-exchange from sodium to calcium ions was made using calcium nitrate tetrahydrate (supplied by Merck). The calcium salt was first dissolved in water, and then carefully added to the dilute NaPA solution. The thus prepared dilute PA solutions contained 5 % active component, i.e. 5 % acrylate. The solutions were pH adjusted to 10.5 with a NaOH solution (mass fraction of 10%) before being added to the pigment slurry, followed by binder addition and additional water to reach a target solid content of 67 %. The coating colours were finally adjusted to pH 8.8. In three of the seven prepared coating colours, the diluted sodium polyacrylate (NaPA) was added in different dose amounts. In one of the formulations (Ref) no additional dispersant was added. In the remaining three formulations the NaCaPA with partial calcium neutralisation was applied as an additive to the pigment slurry.

2.2 Pilot coating

The coating colours were coated on pre-coated woodfree fine paper (Magnostar 80 $g \cdot m^{-2}$ supplied by Sappi). Both sides of the industrially pre-coated base paper were top-coated with approximately 10 $g \cdot m^{-2}$. The papers were coated with a blade coater at a speed of 1 500 $m \cdot min^{-1}$ (Modular Combi Blade (MCB) manufactured by Voith Paper). For additional process parameters see Appendix.

The coated papers were supercalendered (SK 14/12-90 manufactured by Bruderhaus Maschinen GmbH) and passed through 11 nips, each with a linear nip-pressure of 120 $kN \cdot m^{-1}$ and a line speed of nearly 300 $m \cdot min^{-1}$. The temperature of the calender rolls was kept constant at 90 °C and the papers were calendered to reach 69 % gloss (measured with TAPPI Standard T480). Further process parameters can be found in Appendix.

2.3 Full scale printing

The coated papers were printed 4 weeks after being coated with a sheet-fed offset printing press (Manroland R 706 LTTLV supplied by Manroland sheet-fed GmbH, Germany). For more details of the press set-up, please see Appendix.

The printing order was black (K), cyan (C2), magenta (M), yellow (Y), cyan (C5) and cyan again (C6) as shown in Figure 1. Only the cyan printed areas were evaluated.

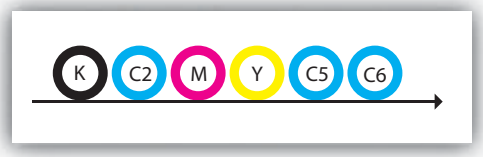

Figure 1: The ink sequence used during the printing trial

The print layout seen in Figure 2 shows a total of six cyan areas, three of which are printed in fulltone (first column) and three areas are printed in 50 % halftone (second column). Each area is printed only once at either C2 (first row in Figure 2), C5 (second row) or C6 (third row), respectively.

The positions of the printing units influence the amount of fount being put onto the paper surface, prior to it being printed. Significantly more fount will be put onto the paper printed at C6 compared to the fount amount on a paper printed at C2. Also the prints from C2 may suffer from back trap mottle caused by the subsequent 4 blanket cylinders (M, Y, C5 and C6), whereas prints from C6 do not risk that as it is the last printing unit in the press.

Table 1: Coating colour formulations

Sample	GCC [pph]	SB latex [pph]	Excess PA dosage [pph]	$[Ca^{2+}]/[A^-]$
Ref	100	11	0	0
0.2 NaPA	100	11	0.2 NaPA	0
0.2 NaCaPA	100	11	0.2 NaCaPA	0.3
0.4 NaPA	100	11	0.4 NaPA	0
0.4 NaCaPA	100	11	0.4 NaCaPA	0.3
0.8 NaPA	100	11	0.8 NaPA	0
0.8 NaCaPA	100	11	0.8 NaCaPA	0.3

Figure 2: Print layout used in the printing trial

A normal fountain feed would be 30–50 %, whereas the feed of 70 % used during most of the trial runs was chosen to show the impact of high moisture, i.e. at very humid conditions, on the print quality. The fountain solution used during the printing process contained two dampening additives, 4 % isopropyl alcohol and 5 % Substifix (supplied by Huber group). For two trial runs using uncalendered papers, a lower more normal fountain feed (30 %) was used. These two uncalendered trial runs were the reference and the coating with 0.8 pph NaCaPA. The rubber blankets were inspected and cleaned between each trial run. No wet pick could be observed for any of the coating formulations.

2.4 Characterisation of the coating colours

The coating colour viscosities for the seven prepared formulations were determined using a Brookfield viscometer at a rotation rate of 20 and 100 min^{-1} using spindle #3. The pH and temperature were held constant at 8.8 ± 0.1 and 27.0 ± 0.6 °C, respectively.

2.5 Characterisation of the paper surface

2.5.1 Topography

The surface topography of the unprinted coated papers was analysed using two measuring devices, Parker Print Surf (PPS (ISO 8791-4:2007), supplied by Lorentzen & Wettre, Sweden) and OptiTopo (supplied by Innventia AB, Sweden). The PPS instrument is sensitive to roughness within the range of 0.6–6.0 μm whereas the OptiTopo can detect smaller variations in the topography than the PPS instrument. The OptiTopo is an optical instrument that determines the topography in μm, given as a standard deviation from a mean plane of the sample using image analysis of two images taken of the exactly same area on the sample. The two images differ only by the illumination direction during the acquisition of the images (Barros and Johansson, 2005). The topography is then computed with a photometric stereo technique (Hansson and Johansson, 1999). Before the topography variations are computed using frequency analysis, a band-pass filter is applied to eliminate both the finest-scale and largest-scale variations. The bandwidth of the filter used was 0.01–0.5 mm.

2.5.2 Contact angles

The apparent contact angle and volume absorption of water on the coating surface were measured using the Fibro-DAT instrument (supplied by Fibro System AB, Sweden). The instrument places a droplet of deionized water onto the sample surface and then records the height and base diameter of the droplet as a function of time, together with the contact angle. The values after 0.5 s are reported. The contact angle measurements were performed 12 months after the coating trial, during which the papers were stored in boxes in a non-conditioned storage room.

2.5.3 Permeability analysis

The permeability of tablets made of compressed and dried coating colour was determined gravimetrically using a permeability apparatus (Schoelkopf, Gane and Ridgway, 2004) developed by Omya International AG, Switzerland. Tablets were formed by filtration of the coating colour under pressure (15 bar). The coating colours analysed were formulated according to those shown in Table 1. The coatings were filtered through a fine membrane filter (0.025 μm) supported by two coarser metal meshes. The time required to form a tablet of a certain height depends both on the solids content of the sample, the water retention properties and the size and packing characteristic of the solid particles in the sample. The tablets obtained had a diameter of 4 cm and a thickness of 1–2 cm was attained. The tablet forming procedure took 3–5 h. The tablets were then dried in an oven (60 °C) overnight.

Before the permeability measurements could be performed, the tablets needed to be further prepared. The dried tablets were cut and ground into blocks, see Figure 3, with a cross sectional area of about 1 cm^2. The blocks were then embedded in resin and left to cure overnight at room temperature. The absorbing

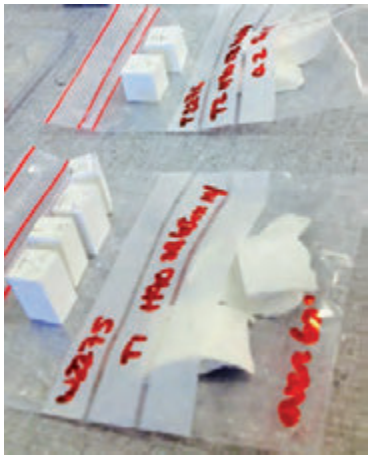

Figure 3: Blocks of compressed coating colour

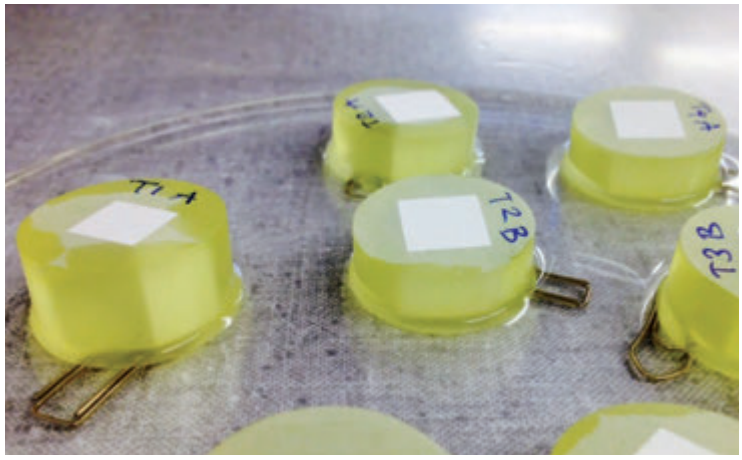

Figure 4: Coating colour blocks embedded in resin and left to imbibe hexadecane

surfaces of the embedded blocks were then carefully ground to ensure full removal of excess resin from the surface. When the resin had dried, the now embedded blocks were placed in a glass dish with hexadecane (ReagentPlus Solvent Grade (99 % purity) supplied by Sigma Aldrich), see Figure 4, and left there until the entire block was saturated with hexadecane, which took roughly one week.

The permeability measurement was performed by placing the embedded sample in the permeability apparatus. Hexadecane was injected into the permeability cell and the sample chamber was then kept pressurised at 7 bar using nitrogen gas. The permeability apparatus was mounted over a micro balance and during the permeability analysis the permeated hexadecane was collected in a sampling dish, placed on the balance, so that the mass of hexadecane as a function of time could be noted (measurements took ~ 5 days). This analysis returned the volume rate of the hexadecane flow, and using Darcy's law (Equation [1]) the permeability, in terms of Darcy's permeability constant (k), could be derived (Schoelkopf, Gane and Ridgway, 2004).

$$Q = \frac{-kA\Delta P}{\eta l} \qquad [1]$$

where Q is the volume flow, k is the permeability constant, A is the cross sectional area, ΔP is the pressure difference, η is the viscosity of the liquid, and l is the length of sample.

2.5.4 Pore structure analysis

The pore structure of the coating colour tablets, generated for the permeability analysis described above, was evaluated. The pore volume intrusion was analysed on 1.5–2.0 g sample material using a Micromeritics Autopore IV mercury porosimeter (Micromeritics Instrument Corporation, Norcross, GA, USA). The mercury porosimetry method is based on the intrusion of the non-wetting liquid mercury into the sample under pressure. The pressure required to intrude mercury into the sample structure is then inversely proportional to the pore size, and therefore this technique yields pore size according to the Young-Laplace equation [2].

$$D = \frac{1}{P} \cdot 4\gamma \cos\theta \qquad [2]$$

where D is the diameter, P is the pressure, γ is the surface tension of mercury, and θ is the contact angle of mercury in contact with the sample.

The maximum applied pressure of mercury was 414 MPa, equivalent to a Laplace throat diameter of 4 nm. The equilibration time at each of the increasing applied pressures of mercury was set to 30 seconds. It is vital that the mercury intrusion measurements be corrected for the compression of mercury, expansion of the penetrometer and compressibility of the solid phase of the sample. This is performed conveniently using the software Pore-Comp (a software program developed by and obtainable from the Environmental and Fluids Modelling Group, University of Plymouth, U.K.), in which the Pore-Comp equation [3] (Gane et al. 1996) is applied:

$$V_{int} = V_{obs} - \delta V_{blank} + \left[0.175(V^1_{bulk})\log_{10}\left(1 + \frac{P}{1820}\right)\right] - V^1_{bulk}(1 - \Phi^1)\left(1 - \exp\left[\frac{(P^1 - P)}{M_{ss}}\right]\right) \qquad [3]$$

where V_{int} is the volume of intrusion into the sample, V_{obs} is the volume of intruded mercury, δV_{blank} is the volume change during blank run, V^1_{bulk} is the sample bulk volume at atmospheric pressure, P is the applied pressure, Φ^1 is the porosity at atmospheric pressure, P^1 is atmospheric pressure, and M_{ss} is the Bulk modulus of the solid sample.

2.6 Characterisation of print quality

2.6.1 Print density

The print density of cyan fulltone areas was measured with a reflection densitometer (Techkon supplied by SpectroDens) which records the amount of light reflected by the studied surface over an exposure wavelength range of 500–520 nm. The densitometer returns the print density as a logarithmic ratio between the light reflected by white (unprinted) paper and the light reflected by the print. The print density reported in this study is the average print density of 10 measurements.

2.6.2 Print gloss

The print gloss at an angle of 75° (according to TAPPI Standard T480 using a ZLR 1050M glossmeter supplied by Zehntner) of cyan fulltone areas was detected and the stated results are an average of 20 measurements.

2.6.3 Uncovered area

The uncovered area (UCA) on printed areas was quantified with the STFI mottling (Johansson and Norman, 1996) image analysis software. The prints are scanned (Perfection v750 Pro scanner with a maximum optical resolution of 4 800 dpi × 6 400 dpi supplied by Epson) and saved as grey-scale images. The software uses light reflectance shown in the grey-scale image. The images are calibrated with respect to reflectance, by determining a reflectance threshold (relative to the mean reflectance level of the image), and UCA is then computed by including all areas with a higher reflectance than the threshold as those contributing to the computed UCA. The resolution of the analysed images was 600 dpi, which represents a pixel size of 42.3 μm. The UCA reported is an average of 10 analysed areas (4.3 cm × 4.3 cm).

2.6.4 Print mottle

The occurrence of print mottle was also evaluated using the STFI mottling software. The software determines print mottle by detecting the spatial change in light reflectance in grey-scale images. The images are calibrated to reflectance and the output data from the mottle analysis is the coefficient of variation (COV) in reflectance, divided into spatial wavelength bands. Values of variation over 1 % are considered to be of importance. Print mottle was analysed on 10 areas (4.3 cm × 4.3 cm) of each sample.

3. Results

3.1 Viscosity of coating colour

The Brookfield viscosity increased upon addition of polyacrylate (PA) dispersant, see Figure 5. Excess dispersant leads to the presence of free water-soluble polyacrylate in the suspension (Loiseau et al., 2005), which leads to induced pigment and binder agglomeration, which is manifested by increased viscosity related primarily to depletion flocculation (Husband, 2000).

The viscosity increase was seen to be higher in the coating formulation where partially calcium neutralised dispersant had been added, in particular at the highest dosage. The detrimental impact of high levels of bound calcium ions on the dispersing effect of polyacrylate has also been shown by Järnström (1993). It is known that calcium ions interact strongly with sodium polyacrylate (Stenius, Järnström and Rigdahl, 1990) during the formation of Ca-polyacrylate complexes which are solu-

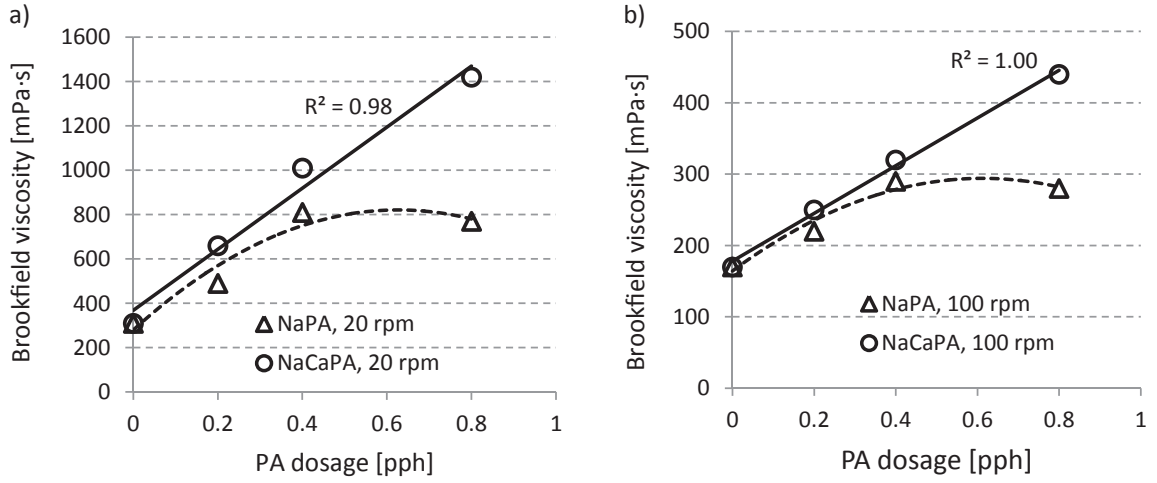

Figure 5: The Brookfield [mPas] viscosity as a function of increasing amounts of NaPA and NaCaPA dosage at a rotation rate of a) 20 rpm and b) 100 rpm

ble at low Ca to PA ratio but form colloidal particles at and above a certain ratio. This ratio, also referred to as seed point, decreases with the polyacrylate concentration (Kamal Alm et al., 2010). It is reasonable to assume that a water-soluble Ca-PA complex gives a lower contribution to the viscosity increase than a water-soluble polyacrylate without Ca since its dissociation is impeded and so the charge density is reduced by incorporating calcium ions. Thus, the stronger viscosity increase in the suspensions where partly calcium neutralised dispersants had been used is likely due to formation of colloidal Ca-PA particles and/or particulate agglomeration. The drop in the viscosity at 0.8 pph NaPA is then expected to be due to a reduction in Ca^{2+} concentration due to the high excess of PA, and thus also a reduction of colloidal Ca-PA particles.

3.2 Properties of the paper surface

The paper surfaces studied here were from the pilot coated series, and both calendered and uncalendered papers were included.

3.2.1 Topography

The different formulations had no impact on the surface roughness, while calendering, as expected, reduced the roughness. The mean values of 10 measurement points on every formulation included in this study, on both calendered and uncalendered surfaces, are given in Table 2.

Table 2: The mean of all surface roughness values measured with PPS and OptiTopo ± standard deviation

Sample	PPS [µm]	OptiTopo [µm]
Calendered	0.59 ± 0.04	0.21 ± 0.04
Uncalendered	1.56 ± 0.11	0.53 ± 0.05

These roughness results match our previous findings (Kamal Alm et al., 2010), where high (0.8 pph) dosage of polyacrylate had no effect on topography. In this study we have confirmed that this is the case also for lower additions. Thus, the aggregation of coating pigments and/or binder, induced by additional polyacrylate, had little or no impact on the surface roughness at the scale measured.

3.2.2 Contact angle

The contact angle between a water droplet and the coated paper surface was analysed using the Fibro-DAT instrument. The average contact angles of 8 droplets from each sample were collected. Relatively small differences in contact angles were obtained, but no reliable systematic change could be observed. The contact angles for the calendered samples varied between 87–92° and for the uncalendered samples it varied between 83–92°, the highest standard deviation for these results being ± 3.

3.2.3 Pore structure and permeability

The porosity of the dried coating colour tablets was determined by mercury porsimetry. This analysis returns the pore volume of the dried coating structures, see Figure 6a and 6b for the NaPA and NaCaPA containing formulations, respectively. Increasing dosage of NaPA resulted in a slight increase in pore size and pore volume. The dosing of NaCaPA, however, had a more complex effect on the pore size and volume distribution of the coating structure. A dosage of NaCaPA with 0.2 pph had the largest effect on the pore size and the most marked increase in pore volume, both of which increased significantly at this dosage. This is because the dispersing effect of polyacrylate sharply deteriorates in the presence of free calcium ions, especially at low excess polyacrylate dose (Järnström, 1993) and the depletion effect dominates. Hence, the flocculation of

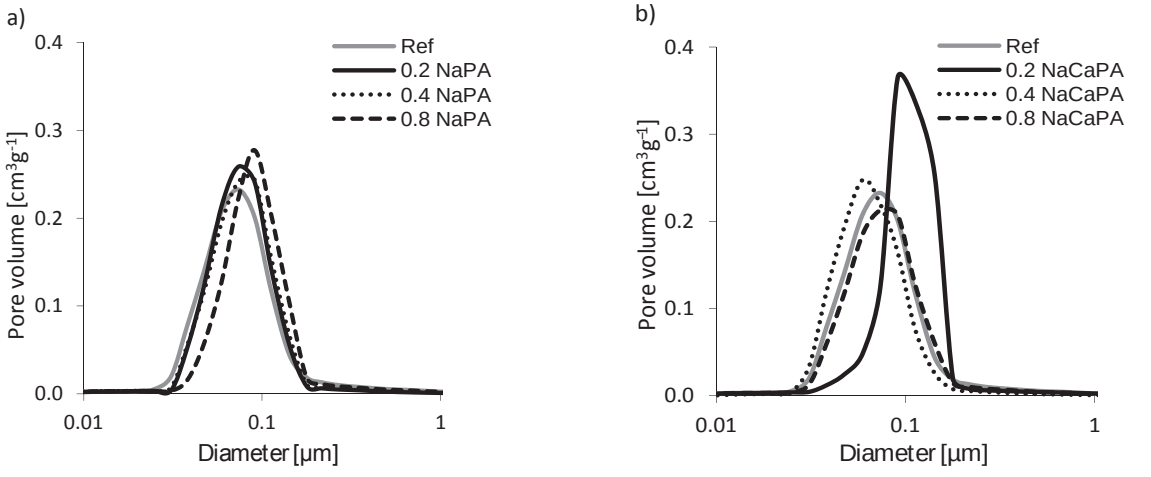

Figure 6: The pore volume [$cm^3 \cdot g^{-1}$] of dried coating colours containing a) increasing amounts of NaPA and b) increasing amounts of NaCaPA

pigments, binder and PA is more severe upon initial excess dosage levels of PA in the presence of Ca^{2+} ion compared to higher PA ratio levels, and the pore size therefore increases. Once the initial flocculation is overcome by increased addition of NaCaPA, the trend from dispersed to further flocculation due to charge density increase follows roughly that of the NaPA (Figure 6b versus Figure 6a).

The liquid permeability of the dried coating colour structures is shown in Figure 7. The permeability of the sample containing excess NaPA was significantly higher than for the ones containing excess NaCaPA, with the exception of the sample with the lowest excess of NaCaPA (0.2 pph). These results coincide with the porosimetry results, where the pore volume and pore size of the sample with 0.2 pph excess NaCaPA was in fact significantly higher than for the other coating formulations.

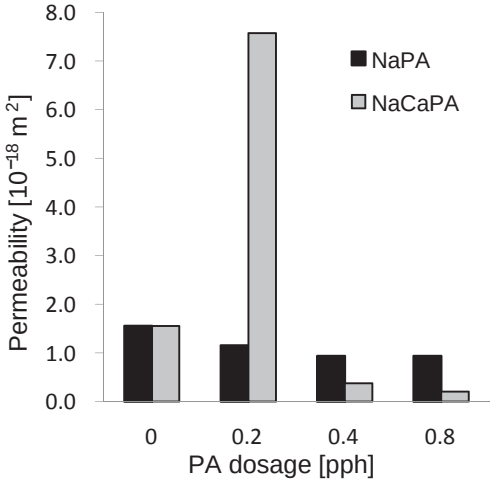

Figure 7: The permeability [10^{-18} m^2] through compressed tablets of ground calcium carbonate

An inspection of the surface structure of the coated papers using SEM showed a significant non-uniformity in porosity with frequent occurrence of compacted/closed areas, in particular for calendered samples, which have been reported previously (Kamal Alm et al., 2015).

3.3 Print quality

Print variability is often seen when printing the cyan colour since the human eye is sensitive to cyan, but also since the cyan inking unit in a multicolour press often is placed early in the print colour order. In addition, cyan is often printed using a relatively low film weight, which leads to a significant visual disturbance when the ink film thickness varies. The results presented here are, therefore, only from cyan printed areas in three different units (C2, C5 and C6) on calendered and uncalendered papers printed with a fountain solution feed of 70 %, which in this study is referred to as the standard high level feed (SF).

Areas printed at C2 have been wetted by fount once (in the K printing unit) before it was printed in C2 and the print will be subjected to four back traps before it leaves the press. Areas printed in C5 have been wetted four times and will be subjected to one back trap before leaving the press, whereas areas printed at C6 have been wetted five times with fountain solution and are not subjected to back trap.

3.3.1 Print density

The average cyan print densities of the seven different papers printed at C2, C5 and C6 were 1.44, 1.24 and 1.43 with standard deviation ± (0.05–0.10) on the calendered and 1.44, 1.39 and 1.41 with standard deviation ± (0.08–0.17) on the uncalendered papers, respectively. Thus, the print density did not vary much between the different papers within each print unit. However, the print density decreased somewhat for almost all calendered trial runs in the 5th print unit (C5) when compared to prints from the two other cyan printing units.

3.3.2 Print gloss

Figure 8 shows print gloss measured at an angle of 75°. Calendered papers returned values around 77 %, while uncalendered gave values around 60 %. The difference between the formulations and print units was small. This was expected since excess PA had no effect on the specular reflecting size component of the coating topography.

3.3.3 Uncovered area

Light microscope images of a print suffering high levels of UCA were acquired. Figure 9 shows an overview image of a print with a high amount of UCA, and a close-up of such an area.

The amounts of UCA on fulltone prints from all cyan print units are shown in Figure 10. The UCA found on prints from C2 was minor in comparison to the quantity of UCA found on prints from the two following print units (C5 and C6). The majority (90 %) of the uncovered areas identified were small (squares of side 1–3 pixels, equal to 42.3–126.9 µm). The average standard deviation of the UCA found in C2, C5 and C6 was ± 0.003, ± 0.092 and ± 0.012 %, respectively, which roughly corresponds to a coefficient of variation of 10 %.

For prints on calendered papers (Figure 10a and 10b), excess dosage of NaPA or NaCaPA, up to 0.4 pph, increased the quantity of UCA. Generally, more UCA was found on the paper coatings with dosed NaCaPA

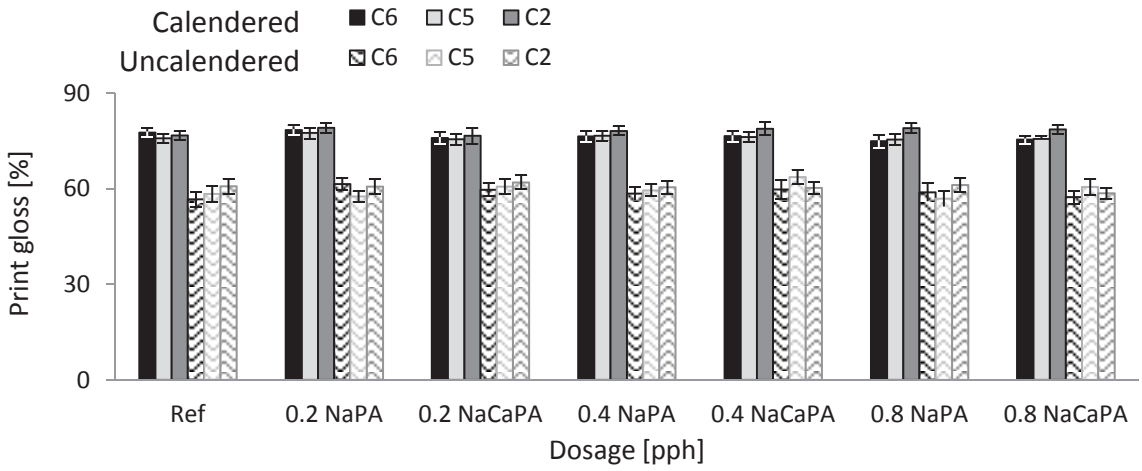

Figure 8: Print gloss at 75°

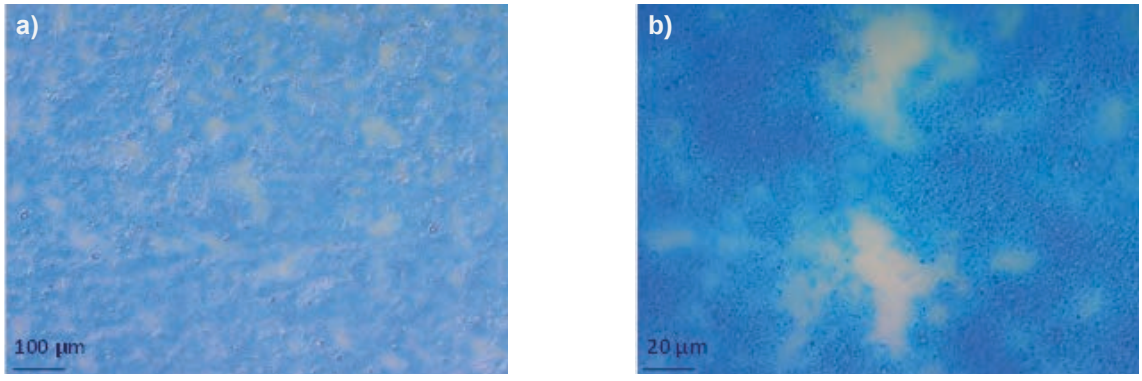

Figure 9: A micrograph image of a print a) with high amounts of UCA and b) UCA adjacent to ink covered areas on a print, at high magnification

compared with NaPA, especially at the lowest excess dosage of 0.2 pph. The highest polyacrylate dosage level, however, is seen not to influence the occurrence of UCA to the same extent as the lower and medium dosage levels.

Also print on uncalendered paper returned higher UCA when additional PA had been added to the coating colour (Figure 10c and 10d). For prints in C5 and C6, maximal UCA was reached already after the lowest dosage of PA. UCA on prints from C2 showed a steady increase with dosage of NaPA and reached a significantly high value at the highest dosage.

The general picture can be summarised as:

- Excess of dispersant leads to an increase in UCA with a maximum at 0.2–0.4 pph excess dispersant.
- The ratio of PA to Ca^{2+} is seen as critical in calcium carbonate-containing coating colours.
- Uncalendered papers showed roughly the same amount of UCA on the fifth and sixth units while calendered papers showed significantly higher UCA on prints from the fifth unit.

3.3.4 Print mottle

The print mottle was measured in two wavelength classes, and the results are given in Figure 11. The larger wavelength class which starts at 0.25 mm shows much higher values than the smaller and most often used wavelength class, which starts at 1 mm. This means that a significant amount of the non-uniformity in print density comes from small sizes, which is reasonable in this case since the majority of the UCA detected was made up from small white spots. Only a small effect on the mottle value related to PA dosage was seen on prints from C2, but a rather limited addition of dispersant had a significant impact on mottle in prints from C5 and C6, where prints from C5 showed the highest values.

Addition of NaCaPA had a more severe impact on the mottle than NaPA, independent on whether the papers were calendered or not. For calendered papers, the print mottle decreased at the highest addition of NaPA or NaCaPA, but this was not as pronounced for the uncalendered papers.

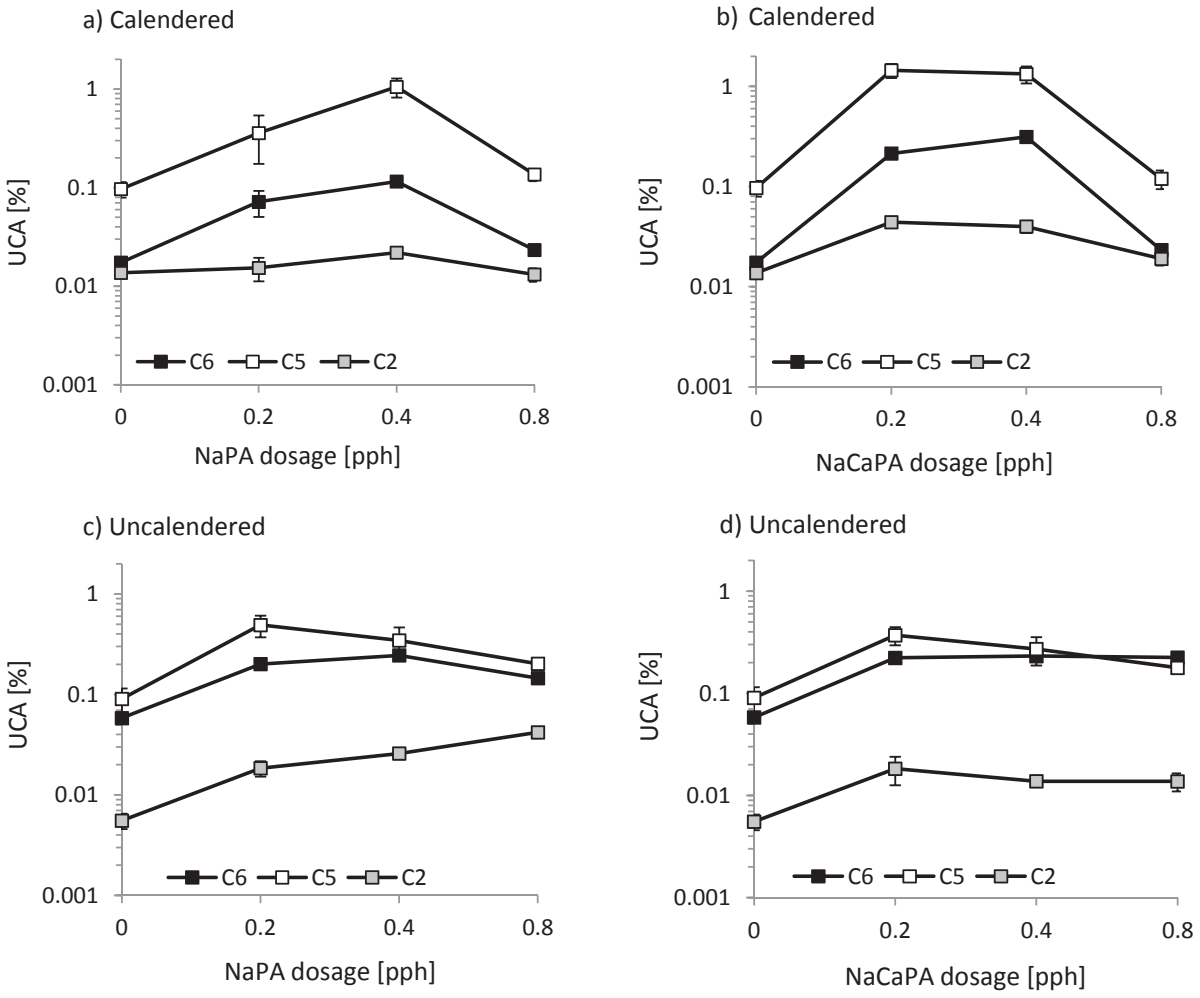

Figure 10: Amount of UCA [%] found on calendered (a, b) and uncalendered (c, d) papers printed at C2, C5 and C6 as a function of NaPA (a, c) and NaCaPA (b, d) dosage [pph], respectively

The print mottle on 50 % halftone prints was also analysed in the same manner as the fulltone prints. Figure 12 shows print mottle of fulltone and halftone prints in the same graph. Increasing PA dosage leads to impaired print quality mainly on prints from C5 and C6. The calendered papers show a clear maximum in print mottle, which indicates the detrimental effect of excess PA dosage when considering print quality. This is also observed on prints on uncalendered papers coated with coating formulations containing NaCaPA.

The detrimental print mottle maximum occurs at higher dispersant dose for the halftone prints compared with the fulltone ones. This endorses the hypothesis that trapped fount can escape sideways slightly better in the halftone print than when trapped under a fulltone ink layer, and so water interference mottle in the halftone is somewhat less severe.

3.4 Impact of fountain feed on UCA and print mottle

For two trial runs the level of fountain feed was reduced from 70 %, which was the standard feed (SF), to 30 %, referred to as reduced feed (RF). Two uncalendered papers were printed, i.e. the reference and the one with 0.8 pph NaCaPA. Figure 13 shows that UCA becomes significantly reduced upon reducing the fountain feed. However, also at the lower feed, the dosage of 0.8 pph NaCaPA still had a significant impact on UCA in prints from C5 and C6, since it was about three times higher compared to the reference. Also the print mottle values were reduced when the fountain feed was reduced, as shown in Figure 14. The mottle values were low also for the paper containing the top level of 0.8 pph NaCaPA. The print quality deteriorating effect of excess PA was, therefore, more evident for the standard (high) fountain level used during these trials.

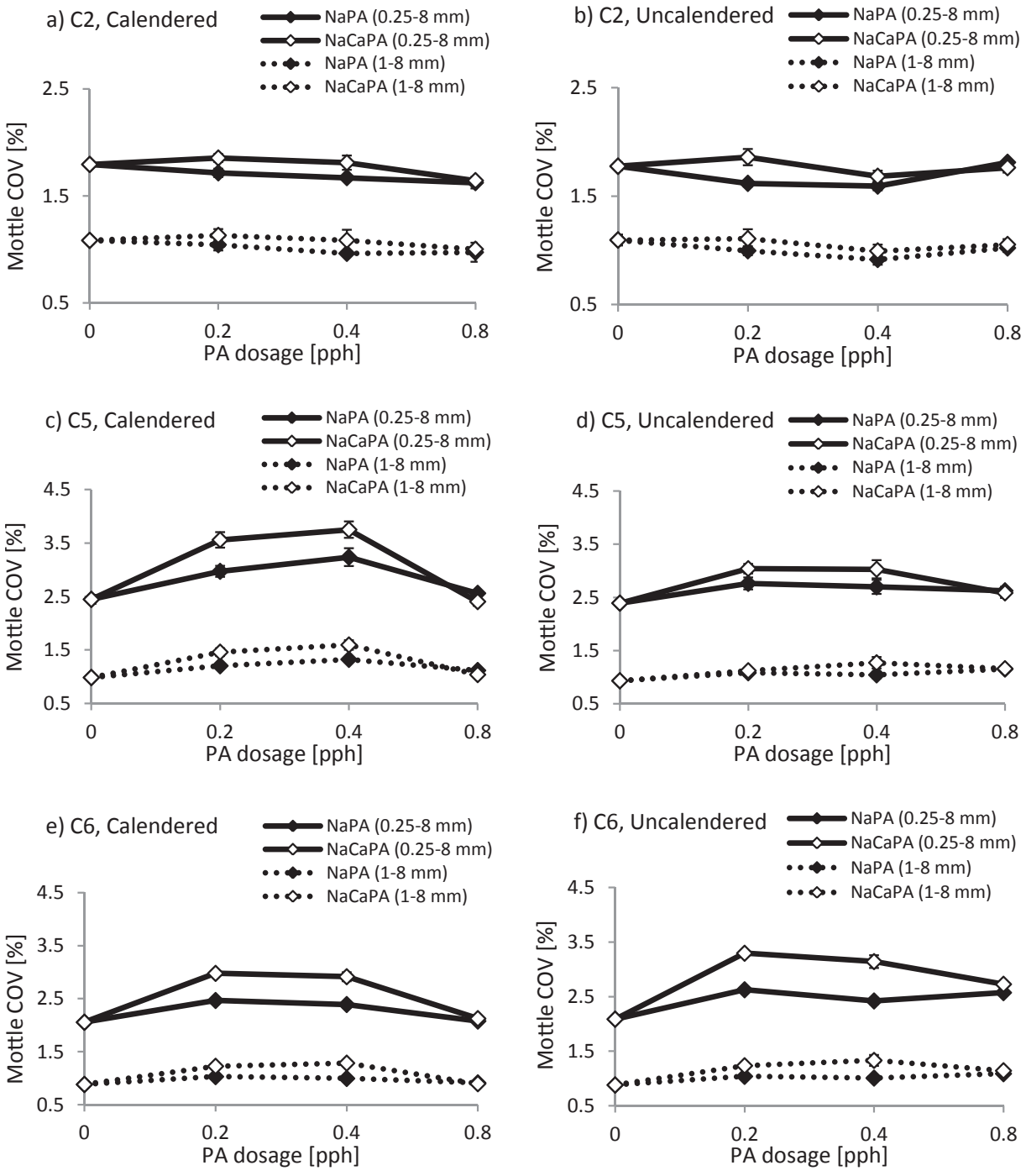

Figure 11a–f: The print mottle COV [%] in two wavelength classes, 0.25–8 mm (solid lines) and 1–8 mm (dashed lines), for the fulltone prints on calendered (left column) and uncalendered (right column) papers from the three print units, where solid symbols are papers with addition of NaPA, while open symbols are with addition of NaCaPA

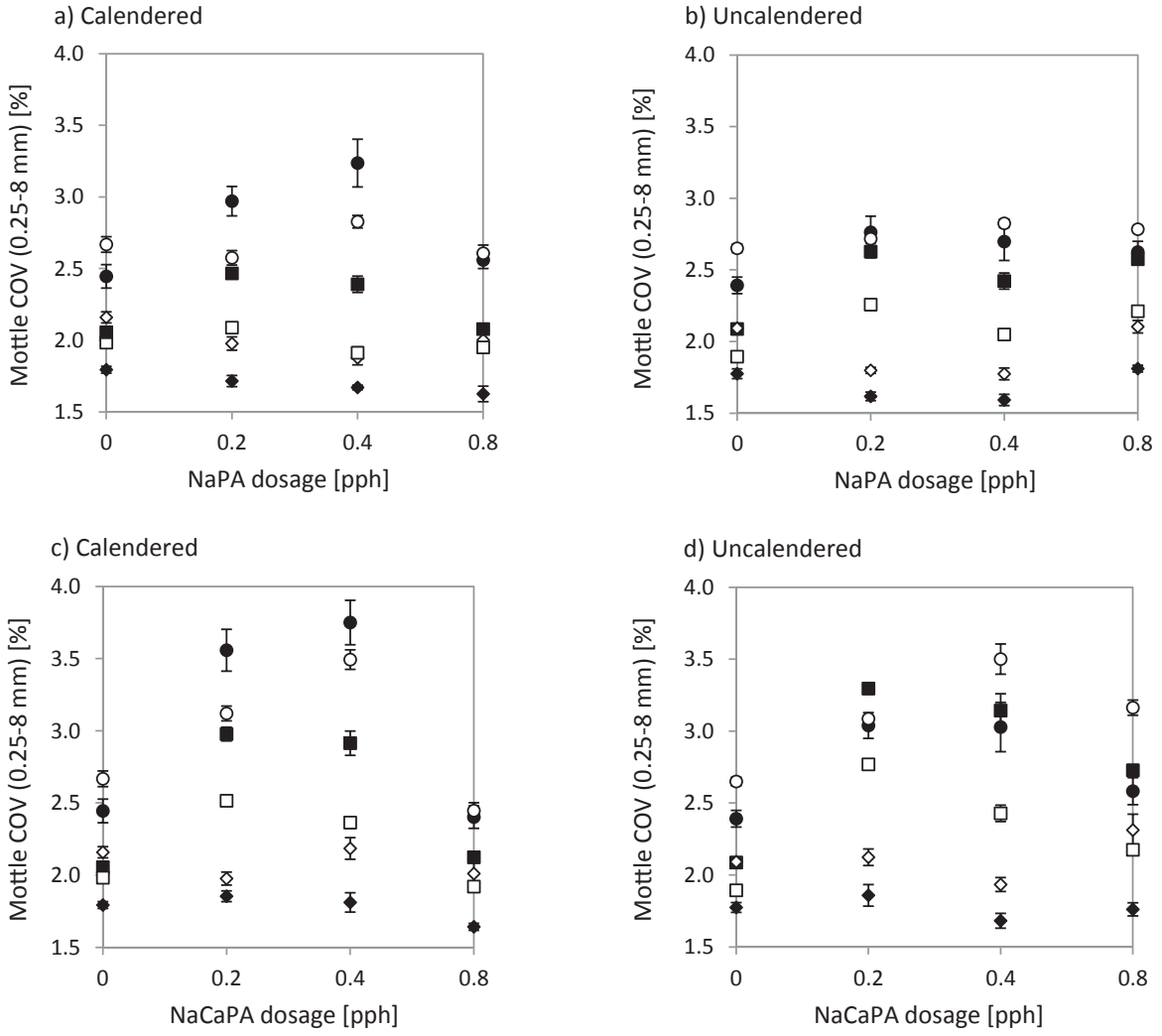

Figure 12a–d: The print mottle COV [%] in fulltone (closed symbols) and halftone (open symbols) on prints printed at C2 (♦ ◊), C5 (● ○) and C6 (■ □), respectively, on a) calendered paper with excess dosage of NaP, b) uncalendered paper with excess dosage of NaPA, c) calendered paper with excess dosage of NaCaPA, d) uncalendered paper with excess dosage of NaCaPA

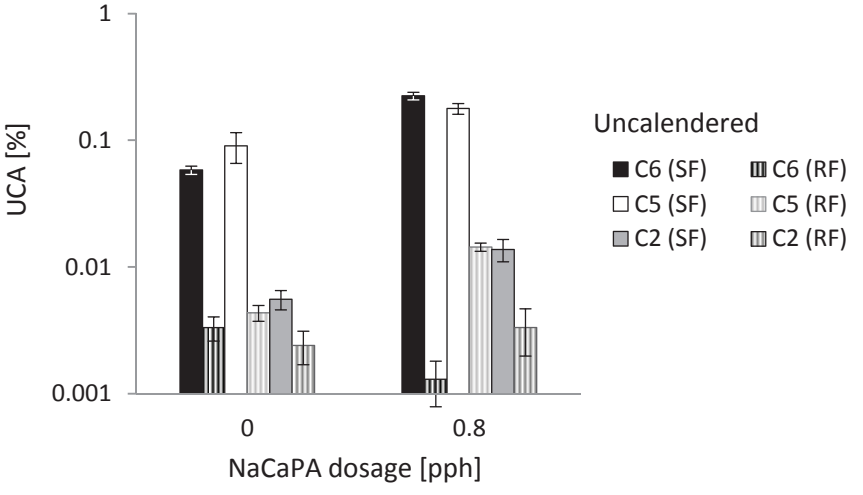

Figure 13: Amount of UCA [%] on fulltone prints printed at C2, C5 and C6, respectively, when two (SF and RF) fountain feed levels were used

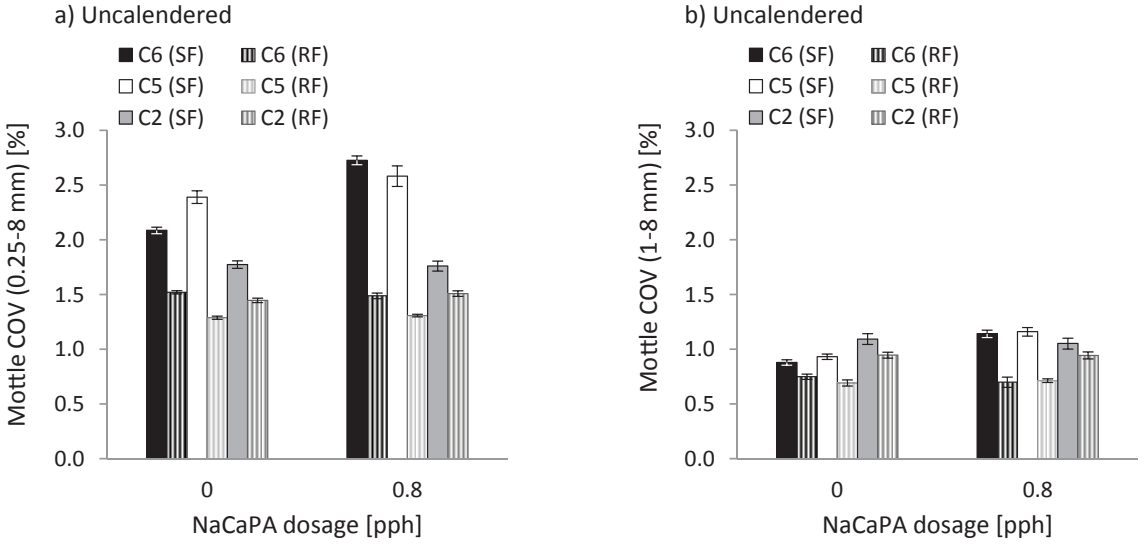

Figure 14: Print mottle COV [%] on fulltone prints printed on uncalendered paper at C2, C5 and C6, respectively, when two fountain feed levels were used, SF (solid bars) and RF (striped bars), for two wavelength classes a) 0.25–8 mm and b) 1–8 mm

4. Discussion

4.1 Coating structure and surface chemistry

The presence of excess NaPA has a significant impact on local pore structure and surface chemistry of the coating layer, and these in turn appear to be key factors for ink adhesion. Compact areas within the surface layer of the coating have been identified (Kamal Alm et al. 2015) and an example of such an area is shown in

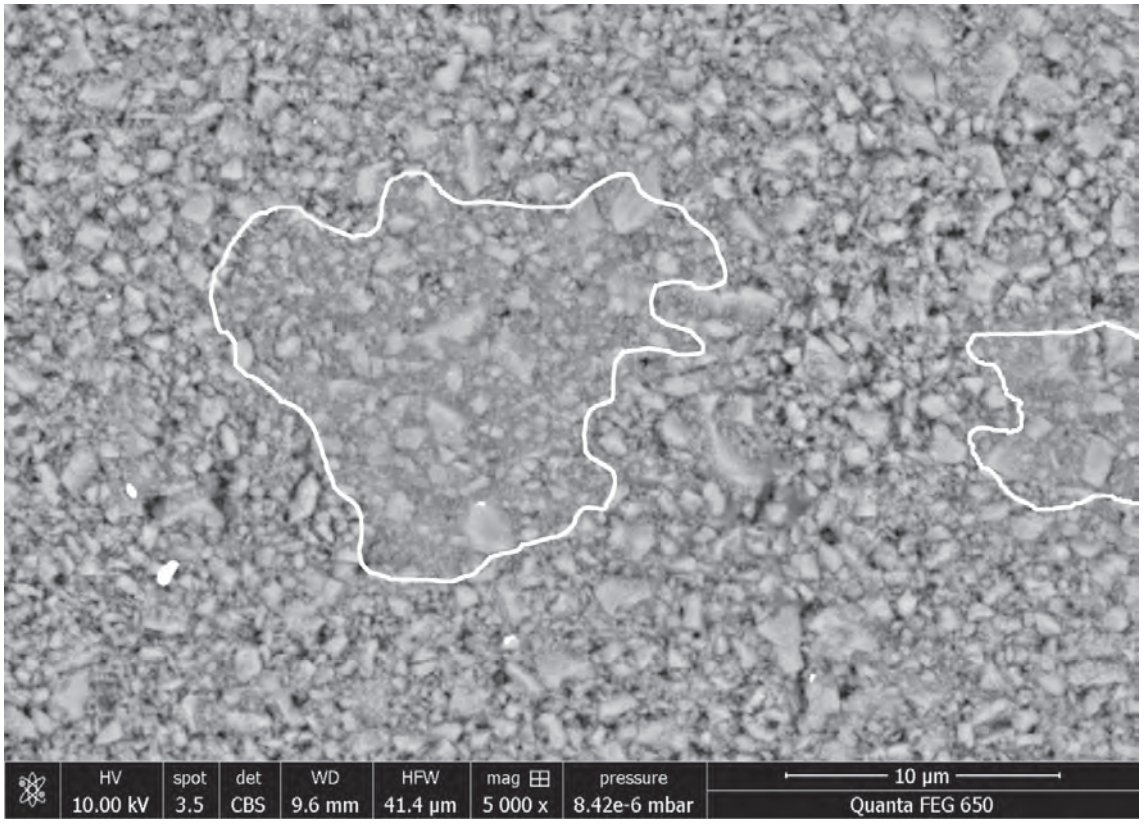

Figure 15: Scanning electron microscope image of an area of the coating with compact spots, which are indicated by the white boundary line

Figure 15. The compact spots occurred more frequently on papers with high amount of UCA and contained more NaPA than open areas. Data on this relation effect have been reported in a recent publication (Kamal Alm et al., 2015), in which focus was given on the relation between paper properties and the ink adhesion failure mechanism, while this paper focuses on the overall printability.

Literature data comparing the surface chemistry of calcite with adsorbed NaPA and that of calcium carbonate coatings with excess dispersants added have shown that adsorption of NaPA makes the surface more hygroscopic, more polar and the pore structure absorbs water faster (Koivula, Kamal Alm and Toivakka, 2011; Kamal Alm et al., 2010). For model systems of freshly cleaved calcite surfaces Koivula, Kamal Alm and Toivakka (2011) showed that the water contact angle on clean calcite surface was around 50°, while it decreased to about 30° for a calcite surface covered by adsorbed NaPA.

The value decreased even further when tested in a more humid environment. The findings were supported by data from vapour sorption isotherms, which showed strong increase in adsorbed vapour when the relative humidity exceeded 50 %. Also reported was the surface energy of calcite with adsorbed NaPA. The total surface energy was 46.8 $mJ \cdot m^{-2}$ with the Lifshitz–van der Waals part being 21.4 $mJ \cdot m^{-2}$ and the acid-base part being 25.5 $mJ \cdot m^{-2}$. The Lifshitz–van der Waals contribution to the surface tension of water is 21.8 $mJ \cdot m^{-2}$ (Fowkes, 1980), which is very close to the value found for an adsorbed layer of NaPA. This suggests that the layer in a moist environment is a mixed layer of water and NaPA. Layers of polyacrylate are indeed both hygroscopic, hydrophilic and polar.

In a coating layer, the situation becomes different since the calcium carbonate surface is not as pure as was studied for the calcite, and one must consider that partially hydrophobic polymer latex with surface active agents has also been added. Moreover, the typical coating layer is microrough, porous and chemically heterogeneous, all of which makes the interpretation of contact angle difficult. In addition, the contact angles of the pilot coated papers were measured some 12 months after coating and cannot be used in the discussion since, amongst many factors, mobile components of the coating migrate to the surface and act to render it hydrophobic (Lindenmark et al., 2010). Instead, we refer to earlier work conducted at our laboratory. These measurements showed a decrease in the advancing water contact angle of 10°, from 86° to 76°. Even though the decrease in contact angle is moderate it has a significant impact on wettability, since the cosine value of the contact angles goes from 0.07 to 0.24. It is the cosine value of the contact angle, which reflects the wettability linearly.

The water absorption, as observed in the contact angle measurements, occurring within the first 8 ms from contact we refer to as "instantaneous absorption", and it was seen to change from 0 to 10 $cm^3 \cdot m^{-2}$ upon introducing 0.8 pph extra polyacrylate. The surface energy of the coated layer, as calculated from the advancing contact angle, was around 44 $mJ \cdot m^{-2}$ and the acid-base part had increased from around 1 to 2.5–3 $mJ \cdot m^{-2}$ upon addition of extra NaPA. This can be seen as a significant increase, since the advancing contact angle, which was used in the calculations, is strongly influenced by the low energy areas of the heterogeneous surface, in this case areas with high amount of latex.

The data for calcite, and the fact that polyacrylate is concentrated within compact areas, suggest that the compact spots may by more polar than the average polarity of the coating layer.

4.2 Ink adhesion failure mechanisms in offset printing

Water on hydrophilic surfaces has a significant importance for ink transfer in offset printing. Non-image areas of the printing plate are hydrophilic and fountain solution is applied to prevent ink adhering to these areas. The mechanism that inhibits the ink adhering to non-image areas was earlier believed to be a result of adhesion failure at the ink/fountain solution interface (Kato, Fowkes and Vanderhoff, 1982). However, the general belief today is that a cohesive split of the fountain solution layer, rather than a weak interface, is what actually prevents ink transfer onto non-image areas during the printing process (McGill, 1977; Shen, Hutton and Liu, 2004).

According to the Stefan equation [4] (Stefan, 1874), the force needed to split a liquid film depends on the splitting velocity, but, more importantly for this application, it is inversely proportional to the third power of the film thickness and proportional to viscosity of the film.

$$\frac{F}{A} = \frac{C\eta v}{t^3} \qquad [4]$$

where F is the force, A is the plate area, C is the constant, η is the viscosity of liquid, v is the velocity at plate separation, and t is the film thickness or distance between plates.

MacPhee (1979) used this as a starting point to discuss ink transfer in offset printing and showed theoretically that for a configuration of non-image area/fountain solution/ink/ink roller, splitting will occur in the ink layer when the thickness of the fount layer is low, but once it exceeds a certain value splitting will occur within the fountain solution film. The critical thickness depends on the viscosities of the two liquids as well as the thickness of the ink film and can be calculated using Stefan's equation. A calculation using industrial-like conditions

suggests that the critical fountain solution film thickness is around 40 to 80 nm, below which ink transfer to the non-image areas of the printing plate is likely to occur. The calculation is based on an ink film thickness of 2 μm and a ratio of ink viscosity to fount viscosity between $2 \cdot 10^4$ and 10^5.

A similar approach can be used for the appearance of spots without ink, i.e. UCA on a moist paper surface due to ink transfer failure, also referred to as ink refusal. UCA is a consequence of areas on the coating surface where the absorption rate of fount is low compared to the printing speed, which results in ink transfer failure. This takes place when the thickness of the fount layer on the paper surface has surpassed the critical thickness required for ink transfer, according to Stefan's equation and the discussion above.

Ink-lift-off, on the other hand, means that the ink has been transferred to the paper, but due to low adhesion to the surface it has been lifted off by the rubber blanket in the subsequent print unit(s). The theoretical explanation for the phenomenon is that ink first is transferred to the paper because the moisture on the paper surface is not sufficient to give ink refusal. The ink is then lifted off by the rubber blanket in the subsequent print nip because the cohesive strength in the ink film has increased, i.e. since the physical state of the ink film has changed, the ink film thickness is now less and its viscosity is higher. The ink film thickness has decreased because the ink film transferred to the paper is thinner than the ink film on the rubber blanket prior to transfer, since splitting normally occurs in the middle zone of the ink film. The ink that is built-up on the non-printing parts of the subsequent rubber blanket(s) has previously been on the paper where ink oil has depleted and its viscosity is higher compared to fresh ink that has been deposited on the printing areas on the rubber blanket from the printing plate.

Given the description above, when ink is transferred to the paper in the 5th unit, the ink film is thick, which results in a cohesive failure within the ink film and thus ink transfer. Subsequently, when this ink meets the rubber blanket in the 6th unit, the ink film is thinner and it joins together with ink on the rubber blanket, which has high viscosity. The cohesive strength of the ink film is now higher. If it is higher than the strength between the paper and the ink film, the ink will be lifted off from the paper and transferred onto the rubber blanket. The strength between the ink film and the paper surface is strongly affected by the coating structure and surface chemistry, e.g. polar character and moisture on the surface, which definitely will have impact on the strength. This effect relies on the large roles being played by permeability and capillarity, respectively, as large connected pores facilitate transport of fountain solution away from the surface only when external pressure is applied in the nip in contrast to closed areas, and finer pores act between units to remove water by their high capillarity. Calendering will thus be critical since it not only smoothens the surface and reduces the pore size, but also induces compacted/closed areas. An excess of dispersant will make the surface more polar, which enhances adsorption, and so retention, of water molecules and formation of water-containing surface layers.

Another phenomenon that occurs in the presence of excess dispersant, not studied independently here but reported by Loiseau et al. (2005), is the formation of colloidal Ca-PA particles. They are formed at moderate excess of polyacrylate but not at high excess due to a too low concentration of calcium ions in solution following the initial chelation by the dispersant at lower dose. These particles may further densify compaction spots under severe calendering within the coating, and so further reduce transport of fount from these spots. Additionally, or alternatively, it is this condition of colloidal CaPA that we see creates the greatest disruption of the coating pore structure, and so a likely non-uniformity in surface chemistry between pigment and binder-rich areas. The fact that UCA is greater when NaCaPA is added compared with NaPA, and the decrease in UCA at high dosages of extra dispersant suggests that the colloidal Ca-PA complex has a significant importance for the overall mechanism.

More details on the mechanism of ink adhesion failure can be found in our previous paper from this printing trial (Kamal Alm et al., 2015). For instance, it was concluded that compact areas in the coating, which have very low permeability after calendering, had a large impact on ink adhesion failure and UCA. In the present study we wanted to investigate whether a value of mean permeability also had an impact on the presence of UCA. Thus, mean permeability was measured and are reported in Figure 7. A comparison between these data and the UCA reported in Figure 10a–d shows no correlation, which suggests mean permeability is not a key factor in determining UCA when initial ink transfer is not impeded. This is logical, since the removal of fount water by hydraulic impression in the printing nip defines the initial ink transfer success, but not the subsequent degree of adhesion. Local spots with low permeability, however, are more detrimental and may be regarded as a severe coating defect.

UCA in prints from C6 can only be due to ink refusal since the 6th unit was the last unit, but UCA in C5 and C2 may be caused by a combination of both ink refusal and ink-lift-off. The data in this paper show that UCA due to ink-lift-off could be as high as 1.5 % on calendered paper, while UCA due to ink-lift-off on uncalendered papers never exceeded 0.5 %. The calendered papers showed low UCA after C6, thus low ink refusal. However, UCA was significant on prints from

C5. Consequently, we consider UCA on the calendered papers to mainly be caused by the ink-lift-off mechanism, and the greater thin layer splitting force generated on the smoother calendered surface.

4.3 Print mottle in different wavelength bands

An ocular inspection of the prints revealed that prints from C5 and C6 had not only white spots but also a small-scale "blurry" pattern of variation in print density. This may be a consequence of water being emulsified into the ink, which dilutes the ink locally and gives a non-uniform distribution of ink pigment on the paper. Thus, water-induced-mottle (WIM) may be divided into two groups; UCA induced mottle and emulsified water induced mottle. In addition, back trap mottle (BTM) may show up in prints from C2 and C5.

Figure 16 show micrograph images of fulltone areas of prints from C5 with low (Figure 16a) and high (Figure 16b) amount of UCA. The mottle value is higher for the print in Figure 15b due to the high amount of UCA. Both prints show small-scale variation and a blurry small-scale pattern is obvious in the left image.

Print mottle is quantified as the print density variation in different wavelength bands. Back trap mottle (BTM) characterised in the wavelength 1–8 mm has previously shown good correlation with perceived unevenness in print density, and, thus, this wavelength band is most often used for quantification of print mottle (Johansson, 1993; Lindberg, Fahlcrantz and Forsgren, 2008). However, there is no information in the open literature about correlations between perceived and measured mottle for water interference mottle (WIM). Since the spots that formed the UCA were small, and the blurriness also appeared to be of small scale, the print mottle was measured not only in the 1–8 mm wavelength band but also in the 0.25–8 mm band in order to capture irregularities of smaller sizes. This larger wavelength interval gave higher values of mottle. Figure 17a shows a diagram where the two mottle values have been plotted against each other for all fulltone prints. The data divide into two linear master curves with very high correlation coefficients and intercepts close to the origin. When only prints on calendered papers were used to calculate the R^2 values, they increased to 0.98 and 0.91 for the upper and lower line, respectively (Figure 17b).

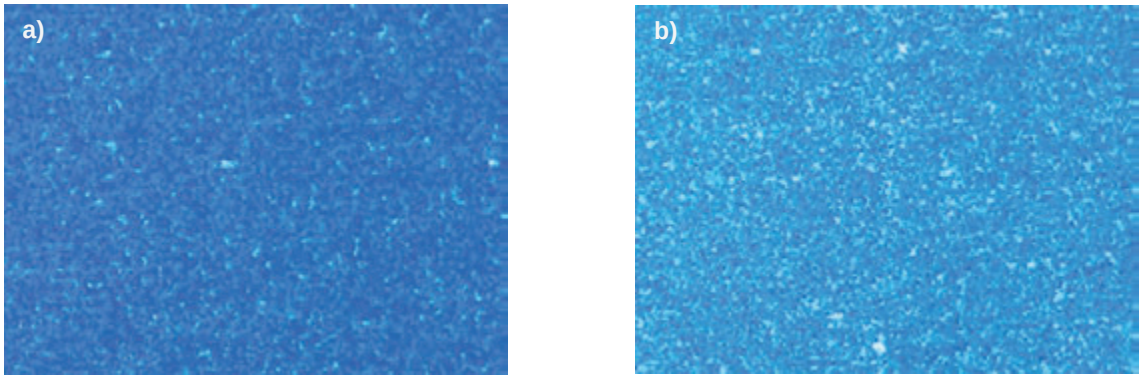

Figure 16: A micrograph image of a mottled print a) with low amount of UCA and b) with high amounts of UCA

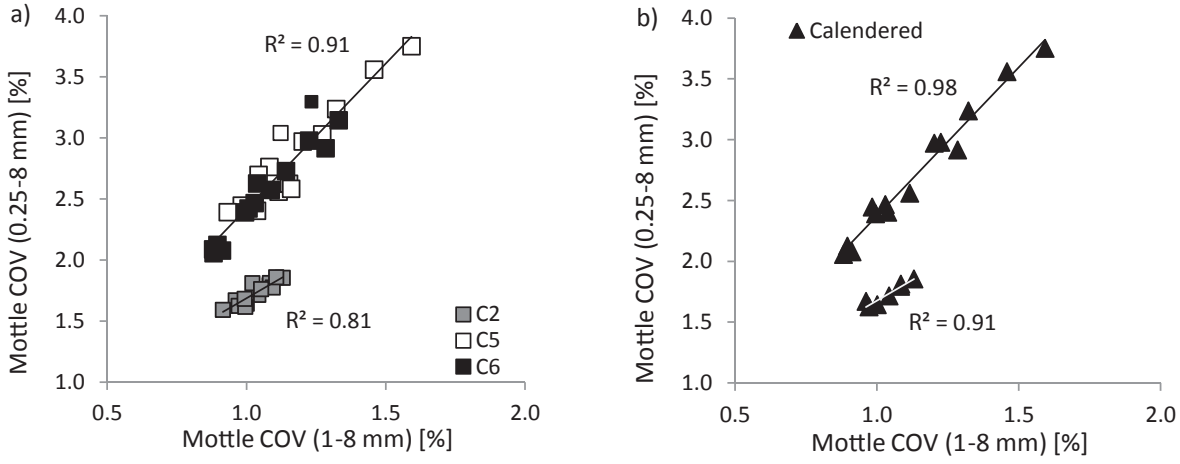

Figure 17: Print mottle COV (0.25–8 mm) [%] as a function of print mottle COV (1–8 mm) [%] on fulltone prints a) on both calendered and uncalendered paper printed at C2, C5 and C6, respectively and b) on calendered paper only

It is indeed initially surprising that the data collect into two lines (Figure 17). All data points in the lower line are from prints in C2, while all the data in the upper line are from prints in C5 and C6 where fountain solution has been in contact with rubber blankets, paper and ink in the earlier print units. The prints in the lower line have a low amount of UCA but the prints from C6 in the lower end of the upper line also have low UCA. Some papers from C2 actually have higher UCA than certain papers from C6 (see Figure 9). Thus, UCA alone cannot fully provide an explanation for the fact that the data form two groups.

In the following, mottle values measured in the larger wavelength band are referred to as "¼^{TO}8-mottle" and mottle values in the shorter wavelength band are referred to as "1TO8-mottle". For the same value of 1TO8-mottle (e.g. 1.0), papers from C5 and C6 have much higher ¼^{TO}8-mottle than papers from C2, about 0.8 units higher. Thus, the small-scale mottle is much higher in C5 and C6 than in C2, which does not only come from UCA.

It is reasonable to assume that the "blurry" ink density pattern which we anticipate to be due to water emulsified into the ink prior to, or during, its transfer to the paper, contributes strongly to small-scale mottle in C5 and C6, and that the mottle in C2 mainly is due to BTM. Furthermore, when the water feed is reduced, the ¼^{TO}8-mottle of the two prints from C2 becomes slightly reduced, from 1.77 ± 0.01 % (mean value of the two prints) to 1.48 ± 0.03 %; also the 1TO8-mottle is slightly reduced, from 1.07 ± 0.02 % to 0.94 ± 0.01 % (see Figure 14. But the impact on the four prints from C5 and C6 is much higher, as the ¼^{TO}8-mottle is reduced from 2.4 ± 0.3 % (mean value of the four prints) to 1.4 ± 0.1 %. In the 1TO8-mottle measured under the same conditions the reduction goes from 1.03 ± 0.14 % to 0.71 ± 0.03 %. The experimental data from C5 and C6 at reduced water feed collect on, or slightly above, the lower line. Thus, it is quite obvious that the upper line collects data were WIM dominates the mottle, while the lower line collects data were BTM dominates. The emulsified water induced mottle (WIM) differs from BTM in the sense that it shows a smaller-scale pattern, and it in turn differs from UCA induced mottle since the light areas have a certain non-zero print density.

A 1TO8-mottle value < 1 is regarded as low. Thus, there was no severe mottle in the C2 prints. On the other hand, the papers with the highest values will touch the limit where there is a need for improvement, and so many of the prints in C5 and C6 classify as suffering from severe mottle.

4.4 Impact of UCA on print mottle

The ¼^{TO}8-mottle values of fulltone prints were plotted as a function of UCA. The results can be seen in Figure 18. Good correlation was obtained on both calendered and uncalendered papers when all papers were included in the plot. A closer look at the correlation coefficients for prints from the different print units (Table 3) shows that high correlation coefficients are obtained for calendered papers printed in the fifth and sixth unit.

Table 3: The collected correlation coefficients (R^2) between mottle and UCA (on a log scale) on prints from the three cyan printing units

Prints from	R^2	
	Calendered	**Uncalendered**
C2	0.44	0.01
C5	0.95	0.51
C6	0.91	0.43
C2, C5 and C6	0.93	0.79

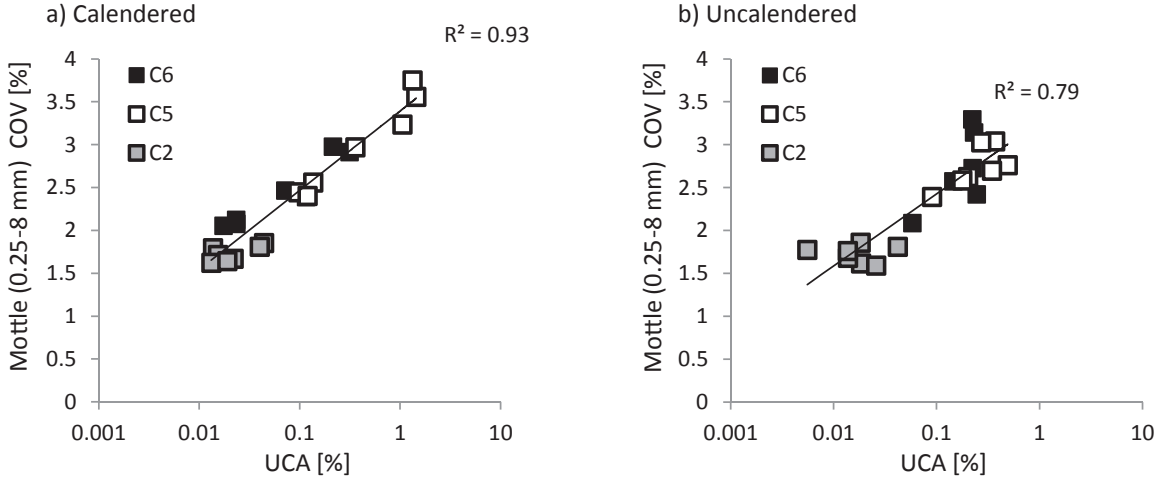

Figure 18: The print mottle COV [%] for the larger wavelength class as a function of UCA [%] on fulltone prints printed at C2, C5 and C6, respectively, a) on calendered paper and b) on uncalendered paper

Prints from the second unit and prints on uncalendered papers do not show the same high correlations. For these prints, other factors besides UCA appear to induce print mottle.

For prints in C2, BTM is regarded to be the dominant mechanism, while for uncalendered papers in C5 and C6 the "blurry" pattern from the water emulsion induced mottle may be a dominant contribution to the mottled print. This seems reasonable since uncalendered papers have a more non-uniform surface topography than calendered papers, which contributes to the transfer of an uneven thickness of the wet ink film.

Local variations in emulsified fount may amplify the variation in ink film thickness after ink setting and drying, in particular if the content of emulsified fount is high on areas where a thin wet film was transferred.

4.5 Correlation between fulltone and halftone mottle

In Figure 19, fulltone mottle is plotted against halftone mottle for all prints on calendered and uncalendered papers. The experimental data are grouped into three series. The series from print unit 5 show almost the same mottle in fulltone as in halftone. Prints from C6, where UCA was only due to ink refusal (WIM), shows higher mottle in fulltone than in halftone. This suggests that ink refusal is lower in halftone, most likely because the water on the paper can be pushed away parallel to the surface when the ink dot meets the paper. This effect may well be enhanced due to higher local pressure in the halftone print, related to the smaller contact area presented by the individual ink dots. Prints from C2 show lower values in fulltone mottle. The mottle in C2 is, as already discussed, not influenced by UCA as is evident from the low correlation coefficients in Table 3.

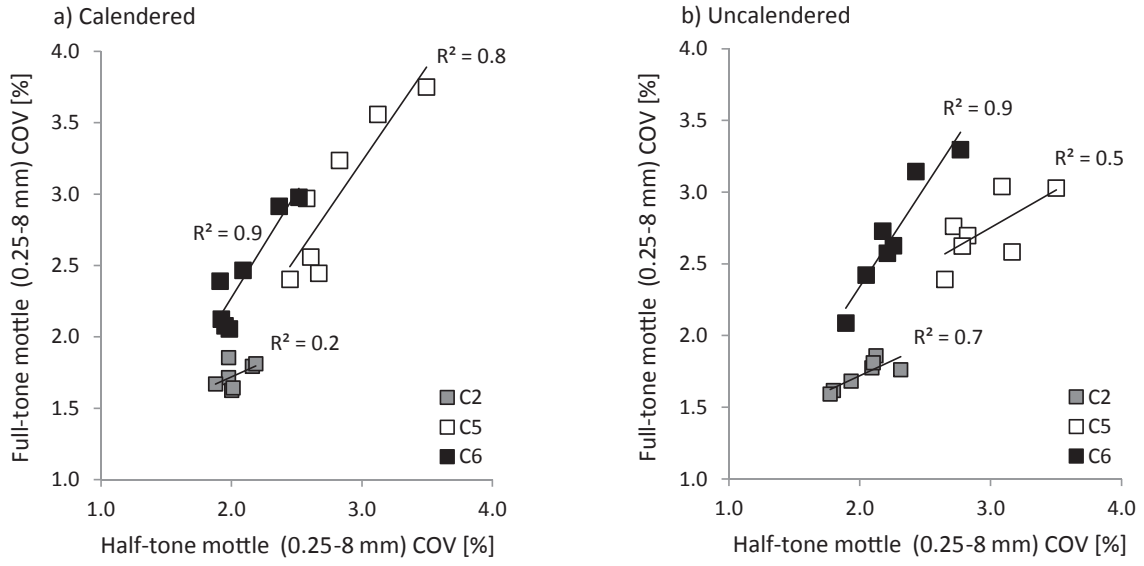

Figure 19: Fulltone mottle COV [%] for the larger wavelength class as a function of corresponding halftone mottle COV [%] on prints printed at C2, C5 or C6, respectively, a) on calendered papers and b) on uncalendered papers

5. Conclusion

The aim of this paper was to gain a solid understanding of the impact of dispersant content in coating colour formulations and of fountain feed level during printing on the quality of offset prints. The papers were pilot coated, calendered and printed during a full scale offset printing trial. Prints from the second, fifth and sixth unit were evaluated. They were printed only once and with cyan. The only difference in coating formulation was the amount of additional dispersant. The papers were evaluated uncalendered and calendered in order to include effects of coating structure. Excess dispersant had a detrimental effect on the printing quality. This was more pronounced at high fountain feed levels and for calendered papers.

The work showed that for prints from the fifth and sixth unit where the paper had been subjected to fount a number of times from the previous nips, the print mottle was dominated by WIM, which showed a more fine-scaled pattern compared to BTM. WIM was strongly influenced by white spots in the print, where the ink adhesion had failed. Beside the white spots, WIM showed a small-scale blurry pattern of variation in print density, which we concluded to be due to fount emulsified into the ink.

When the fount feed was reduced, the WIM character of the mottled prints from the fifth and sixth units became much reduced.

The white spots in the print are referred to as UCA and were due to a failure of the ink–paper adhesion.

We identify two origins of this failure:

- Ink-transfer failure, also referred to as ink refusal, a well-known phenomenon.
- Ink-lift-off failure, which means that the ink initially was transferred to the paper but was removed in a subsequent print unit. This mechanism appeared to be dominant for calendered papers with excess of dispersant. This is a newly reported phenomenon and further details are available in a recent report (Kamal Alm et al., 2015).

The adhesion failure, and thus formation of UCA, occurred in low amounts in absence of additional dispersant and at low water feed on both calendered and uncalendered papers. It is strongly influenced by addition of excess dispersant, water feed and calendering. Increases of 10 to 100 times were observed. This was explained by the formation of a more hydrophilic surface induced by the dispersant, which increases the susceptibility of water molecules to become retained at the outermost surface layer, together with a disruption of coating structure and inhomogeneity through flocculation, which in turn is strongly dependent on the calcium ion to polyacrylate ratio, and formation of non-uniform compact areas induced by calendering, which reduces the transport of free water from the surface to the interior of the coating.

In the light of these findings, it can be concluded that the practice of post-adding excess anionic dispersant to combat the coater runnability-damaging effects of calcium ion release by acidic shock in calcium carbonate containing coating formulations, for example following addition of low pH binders during coating makedown or in the case of prolonged high levels of anaerobic microbiological contamination, is generally highly contraproductive in respect to subsequent print quality.

Acknowledgment

This study was financially supported by Omya International AG and Innventia AB, and their contributions are thankfully acknowledged. Norbert Gerteiser, Maurizio Sturzo and Oliver Grossmann, amongst others, are greatly thanked for the coordination of and the assistance during both the pilot coating trial and the printing trial.

References

Aspler, J., 2006. Ink-water interactions in printing: An update review. In: *9th Tappi Advanced Coating Fundamental Symposium 2006 Proceedings*, February 2006, Åbo, Finland, pp. 117–146.

Barros, G.G. and Johansson, P.-Å., 2005. The OptiTopo technique for fast assessment of paper topography – limitations, applications and improvements. *Journal of Imaging Science and Technology*, 49(2), pp. 170–178.

Fadner, T.A. and Doyle, F.J., 1985. Real-time rates of water pickup by lithographic inks. In: *TAGA 1985 Proceedings*, pp. 309–327.

Fowkes, F.M., 1980. Surface effects of anisotropic London dispersion forces in n-alkanes. *The Journal of Physical Chemistry*, 84(5), pp. 510–512.

Gane, P.A.C., Kettle, J.P., Matthews, G.P. and Ridgway, C.J., 1996. Void space structure of compressible polymer spheres and consolidated calcium carbonate paper-coating formulations. *Industrial and Engineering Chemistry Research*, 35(5), pp. 1753–1764.

Hansson, P. and Johansson, P.-Å., 1999. A new method for the simultaneous measurement of surface topography and ink distribution on prints. *Nordic Pulp & Paper Research Journal*, 14(4), pp. 315–319.

Husband, J.C., 2000. Interactions between ground calcium carbonate pigments and polymer latices. *Nordic Pulp & Paper Research Journal*, 15(5), pp. 382–386.

Isoard, J.C., 1983. Ink transfer and retransfer – mottling and offset picking of coated papers. In: *Tappi Coating Conference 1983 Proceedings*, San Francisco, USA, pp. 143–153.

Johansson, P.-Å., 1993. Print mottle evaluation by band-pass image analysis. In: W. H. Banks, ed., *Advances in Printing Science and Technology: Proceedings of the 22nd International Research Conference of Iarigai*, Munich, Germany, Pentach Press, 22, pp. 403–413.

Johansson, P.-Å. and Norman, B., 1996. Methods for evaluating formation, print unevenness and gloss variations developed at STFI. In: *Tappi Process and Product Quality Control Conference 1996 Proceedings*, Tappi Press, Atlanta, p. 139.

Järnström, L., 1993. The polyacrylate demand in suspensions containing ground calcium carbonate. *Nordic Pulp & Paper Research Journal*, 8(1), pp. 27–33.

Kamal, H., Ström, G., Schoelkopf, J. and Gane, P.A.C., 2010. Characterization of ink-paper coating adhesion failure: effect of pre-dampening of carbonate containing coatings. *Journal of Adhesion Science and Technology*, 24(3), pp. 449–469.

Kamal Alm, H., Ström, G., Karlström, K., Schoelkopf, J. and Gane, P.A.C., 2010. Effect of excess dispersant on surface properties and liquid interactions on calcium carbonate containing coatings. *Nordic Pulp & Paper Research Journal*, 25(1), pp. 82–92.

Kamal Alm, H., Ström, G., Schoelkopf, J. and Gane, P.A.C., 2015. Ink-lift-off during offset printing: A novel mechanism behind ink-paper coating adhesion failure. *Journal of Adhesion Science and Technology*, 29(5), pp. 370–391.

Kato, Y., Fowkes, F.M. and Vanderhoff, J.W., 1982. Surface energetics of the lithographic printing process. *Industrial & Engineering Chemistry Product Research and Development*, 21(3), pp. 441–450.

Kipphan, H., 2001. *Handbook of print media*, Heidelberg, Germany: Springer, pp. 52–53, 206, 211.

Koivula, H., Kamal Alm, H. and Toivakka, M., 2011. Temperature and moisture effects on wetting of calcite surfaces by offset ink constituents. *Colloids and Surfaces A: Physiochemical and Engineering Aspects*, 390(1–3), pp. 105–111.

Lidenmark, C., Forsberg, S., Norgren, M., Edlund, H. and Karlsson, O., 2010. Changes with aging in the surface hydrophobicity of coated paper. *Tappi Journal*, 9(5), pp. 40–46.

Lie, C. and Kolseth, P., 2007. Aspects of water-induced mottle when printing on coated paper in sheet-fed lithographic offset. In: N. Enlund and A. Defrusne, eds., *Advances in Printing and Media Technology: Proceedings of the 34th International Research Conference of Iarigai*, Grenoble, France, 34, pp. 59–67.

Lindberg, S., Fahlcrantz, C.-M. and Forsgren, G., 2008. Making subjective assessments objective – A mottle ruler for calibration of panel assessments of perceived print mottle. *PaperCon08 Tappi/PIM/Coating conference Proceedings*, Dallas, USA, pp. 39–52.

Loiseau, J., Ladavière, C., Suau, J.M. and Claverie, J., 2005. Dispersion of calcite by poly(sodium acrylate) prepared by reversible addition-fragmentation chain transfer (RAFT) polymerization. *Polymer*, 46(19), pp. 8565–8572.

MacPhee, J., 1979. An engineer's analysis of the lithographic printing process. *TAGA 1979 Proceedings*, pp. 237–277.

MacPhee, J. and Lind, J., 1991. Measurement of ink film thicknesses printed by the litho process. *TAGA 1991 Proceedings*, pp. 550–573.

McGill, W.J., 1977. Adhesion and failure of organic coatings. *Journal of the Oil and Colour Chemists Association*, 60(4), pp. 121–126.

Ozaki, Y., Bousfield, D.W. and Shaler, S.M., 2008. Characterization of coating layer structural and chemical uniformity for samples with back-trap mottle. *Nordic Pulp & Paper Research Journal*, 23(1), pp. 8–13.

Plowman Sandreuter, N., 1994. Predicting print mottle: A method of differentiating between three distinctively different types of mottle: back-trap mottle, water sensitive mottle and wet ink trapping mottle. *Tappi Coating Conference 1994 Proceedings*, pp. 211–228.

Purfeest, R.D. and Van Gilder, R.L., 1991. Tall-edge picking, back-trap mottle and fountain solution interference of model latex coatings on a six-color press predicted by laboratory tests. *Tappi Coating Conf. 1991 Proceedings*, Atlanta, GA, pp. 146–472.

Rajala, P. and Koskinen, T., 2004. Experimental and statistical investigation of drying effects on coated offset paper quality. *Tappi Journal*, 3(7), pp.19–25.

Schoelkopf, J., Gane, P.A.C. and Ridgway, C.J., 2004. Observed non-linearity of Darcy-permeability in compacted fine pigment structures. *Colloids and Surfaces A: Physicochemical and Engineering Aspects*, 236(1–3), pp. 111–120.

Shen, W., Hutton, B. and Liu, F., 2004. A new understanding on the mechanism of fountain solution in the prevention of ink transfer to the non-image area in conventional offset lithography. *Journal of Adhesion Science and Technology*, 18(15–16), pp. 1861–1887.

Shen, Y., Bousfield, D.W., Van Heiningen, A. and Donigian, D., 2005. Linkage between coating absorption uniformity and print mottle. *Journal of Pulp and Paper Science*, 31(3), pp. 105–108.

Stefan, J., 1874. Versuche über die scheinbare Adhäsion (Experiments on apparent adhesion). *Sitzungsberichte der Mathematisch-Naturwissenschaftlichen Klasse der Kaiserlichen Akademie der Wissenschaften*, LXIX, Part II, pp. 713–735.

Stenius, P., Järnström, L. and Rigdahl, M., 1990. Aggregation in concentrated kaolin suspensions stabilized by polyacrylate. *Colloids and Surfaces*, 51, pp. 219–238.

Ström, G. and Gustafsson, J., 2006. Physical and chemical drying in sheet-fed offset printing on coated paper. *Professional Papermaking*, 2, pp. 72–77.

Ström, G.R. and Karathanasis, M., 2008. Relationship between ink film topography and print gloss in offset prints on coated surfaces. *Nordic Pulp & Paper Research Journal*, 23(2), pp. 202–209.

Ström, G. and Madstedt, S., 2009. Water induced irregularity of halftone dots and its impact on print mottle. In: N. Enlund and M. Lovreček, eds., 2009, *Advances in Printing and Media Technology: Proceedings of the 36th International Research Conference of Iarigai*, Stockholm, Sweden, 36, pp. 353–362.

Tåg, C.-M., Toiviainen, M., Juuti, M. and Gane, P.A.C., 2010. Dynamic analysis of temporal moisture profiles in heatset printing studied with near-infrared spectroscopy. *Measurement Science and Technology*, 21(10), pp. 105602–105613.

Tåg, C.-M., Toiviainen, M., Juuti, M., Ridgway, C.J. and Gane, P.A.C., 2011. Online detection of moisture in heatset printing: The role of substrate structure during liquid transfer. *Industrial & Engineering Chemistry Research*, 50(8), pp. 4446–4457.

Xiang, Y., Bousfield, D.W., Coleman, P.S. and Osgood, A., 2000. The cause of back-trap mottle: Chemical or physical? *Tappi Coating Conf. 2000 Proceedings*, Tappi Press, Atlanta, GA, pp. 45–58.

Xiang, Y., Bousfield, D.W., Hassler, J., Coleman, P. and Osgood, A., 1999. Measurement of local variation of ink tack dynamics. *Journal of Pulp and Paper Science*, 25(9), pp. 326–330.

Appendix

Coating process

Coating application parameters

Coater: Blade coater Modular Combi Blade (MCB) manufactured by Voith Paper The following trial order was used during the coating process: Ref, 0.2 NaPA, 0.4 NaPA, 0.8 NaPA, 0.2 NaCaPA, 0.4 NaCaPA and 0.8 NaCaPA.	
Jetflow:	
Jet gap	0.9 mm
Jet angle	37.72°
Jet position	8.03 mm
Beam angle	33.04°
Blade configuration:	
Blade thickness	0.38 mm
Blade tip angle	30°
Blade extension	16 mm
IR drying: 15 rows of IR were used with a capacity of 510 kW	
Air drying:	
Hood 1	
Air temperature	142 ± 7 °C
Hood pressure	13 ± 3 mbar
Hood 2	
Air temperature	210 ± 18 °C
Hood pressure	14 ± 2 mbar
Hood 3	
Air temperature	128 ± 5 °C
Hood pressure	18 ± 4 mbar

Calendering process

Calender parameters

Supercalender: SK 14/12-90 manufactured by Bruderhaus Maschinen GmbH	
No. nips	11
Speed	300 $m \cdot min^{-1}$
Pressure	120 $N \cdot mm^{-1}$
Temperature	90 °C

Printing trial setups
Print press parameters

Press: Manroland R706 LTTLV manufactured by Manroland sheet-fed GmbH The calendered papers were printed first followed by the uncalendered papers. The following trial order was used: 0.8 NaPA, 0.8 NaCaPA, 0.4 NaPA, 0.2 NaPA, Ref, 0.4 NaCaPA and 0.2 NaCaPA.	
Plates	Agfa Alura, N30 Web, CTP negative
Speed	8 000 sheets/hour
Ink parameters:	
Ink sequence	(K, C2, M, Y, C5, C6)
Ink supplier	Epple Druckfarben
Ink series	ÖkoPlus
Fountain solution parameters:	
pH	5.6
Conductivity	1.228 $\mu S \cdot cm^{-1}$
Isopropyl level	4 %
Additives	5 % Substifix MGA 836509 (Huber Group)
Temperature	12.8 °C
Powder	Grafik Hitronic 3000